Transcription of atomic scale screw dislocation of silicon carbide crystal to X-ray vortex wave field

Various spiral structures are ubiquitously observed in nature, such as in DNAs, which comprise two chains that form a double helix. In industrial functional materials, such as silicon carbide (SiC) crystals used in high-power electronic devices, the density of threading screw dislocations (TSDs) must be reduced to achieve the desired performance [1]. Therefore, an efficient method is required to precisely measure the density of TSDs on SiC crystals.

We devised a method to transcribe the atomic-scale structure of screw dislocations in an X-ray vortex wave field in the reciprocal space. X-ray vortices are ideal phase markers with phase anomalies of 2π or multiples of 2π phase ambiguity with a complete zero intensity at the center [2,3], and can be used for novel dichroism, quantum communications, or even super-resolution imaging (refer to [2]). The formation of the X-ray vortex wave field was confirmed by an X-ray simulation in the kinematical diffraction regime, where the severe multiple diffraction effect was minimized, and was verified using a SiC crystal as reported in [4]. These results provide a novel direction for the development of crystal X-ray optical components.

Conventionally, the evaluation of crystalline dislocations in a large field of view has been performed using X-ray topography, which is unsuitable for a quantitative discussion of the lattice plane around the dislocations. To overcome this problem, we propose a method of X-ray two-beam topography, by which we can determine the phase at the detector plane that is directly related to the deformation of the lattice planes around dislocations. The measurement was performed in the kinematical diffraction regime with a relatively large offset angle from the Bragg peak to overcome the X-ray multiple diffraction effect inside the crystal. This simplified the computer simulations for calculating the phase shift by the Bragg reflection around the TSDs. Our method will be useful because of the relaxed sample size constraint, with a field of view of up to the millimeter scale, of bulk crystalline specimens and will play a complementary role to other high spatial resolution measurements, such as transmission electron microscopy and Bragg coherent diffractive imaging.

For the two-beam topography experiment, we utilized a large and thick bulk 4H–SiC wafer with dimensions of $10\times10\times0.2$ mm^3 containing TSDs. Low-energy electron-channeling contrast images were captured on one of the TSDs under the focused condition, where a spiral pattern was clearly observed (Fig. 1(a)). The X-ray topograph shows that the core of the TSD appears dark under Bragg conditions. We performed a simulation in the kinematical diffraction regime of the Bragg-reflected X-ray wave field downstream of a SiC crystal containing a TSD, as shown in Fig. 1(b). The simulated result showed destructive interference of the Bragg-reflected beam and the generation of an X-ray vortex wave field in reciprocal space (Fig. 1(b)).

To measure the phase distribution in the reflected wave downstream of a SiC crystal, we constructed an X-ray wavefront-dividing interferometer using 7.71 keV X-rays at an undulator beamline, SPring-8 **BL29XUL**, where an X-ray beam is one-dimensionally focused in the vertical direction. X-rays passed through a 10-μm-width slit at the focal plane, which worked as a stable source. We used a parabolic mirror in the transport channel of BL29XUL. The wavefront-dividing two-beam X-ray interferometer was realized with a diamond prism at L_2 = 44.3 m from the slit, which refracted a part of the wave field in the vertical direction.

One of the wave fields irradiates an offset position from the center of the TSD and works as a reference wave. This wave field was approximated as a plane wave, whereas the other wave field irradiated the center of the TSD and received a specific phase shift (Fig. 2). The grazing incidence angle on the prism was set to be approximately 17° to realize the refraction angle of $\Delta\theta_r$ = 38 μrad and the interference fringe spacing of $d_f = \lambda/\Delta\theta_r$ = 4.2 μm, resolvable by our X-ray image sensor. The distance between the prism and crystal was L_3 = 3.6 m to realize the width of the interference region, $L_3\Delta\theta_r$ = 140 μm, large enough to

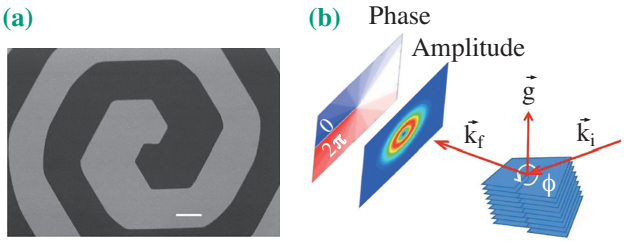

Fig. 1. **(a)** Low-energy electron channeling contrast image of one of the TSDs, where a spiral pattern is clearly observed. The scale bar is 1 μm. **(b)** Summary of the kinematical diffraction simulation. k_i & k_f are incident & exit waves and ϕ is the azimuthal angle around TSD on SiC (0004) plane. The calculated amplitude and phase of the X-ray Bragg reflected wave field from the crystal are shown on the left, exhibiting a donut intensity profile and a spiral phase distribution with a phase jump of 2π.

cover the lattice planes around the TSD.

On the other hand, the Bragg reflection of the SiC crystal occurred in the horizontal direction (Fig. 2). Interferograms are recorded by setting the crystal at an off-Bragg condition of $\Delta\theta$ = 10″, with the measured reflectivity of 5.5% compared to the Bragg peak. Under these conditions, multiple diffraction effects were negligible.

Interferograms obtained using this setup are shown in Fig. 3(a). The bright lines of interferogram bridging the dark line showed two Y-shaped fork patterns with reversed orientations, separated by the amount of shear of $L_4\Delta\theta_r$ (see Fig. 2). This indicates that an X-ray vortex with a topological charge of one was formed in the Bragg reflected wave field. This agrees well with the simulation results for the kinematical diffraction regime shown in Fig. 3(b). In addition, it shows that our two-beam topography enabled us to quantitatively derive the phase shift by Bragg reflection from the areas around the TSD, as predicted by our simulation. Special attention should be paid to the darkened and brightened areas on the fringes, indicated by the upper and lower green dotted lines in Fig. 3(a), extending upward and downwards from the image center, respectively, which likely contain the contributions of basal plane dislocations. The dark centers of the vortices are contained around the image center.

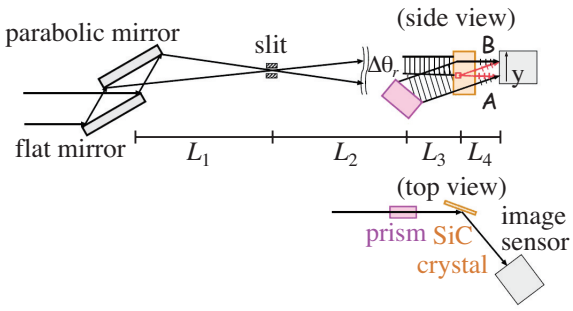

Fig. 2. Schematic diagram of a wave-front dividing two-beam interferometer with a diamond prism splitter. The interference fringes are formed at the overlap of X-rays due to the refraction angle $\Delta\theta_r$ by the prism. The images of TSDs in the interferogram are formed at positions A and B.

Most of the TSDs were accompanied by basal-plane dislocations within the sample.

In conclusion, we proved that the two-beam topography method enables the detection of threading screw dislocations in a large field of view, and we predict that it will play an important role in clarifying the distribution and network of these dislocations and finding methods to significantly reduce them in the near future.

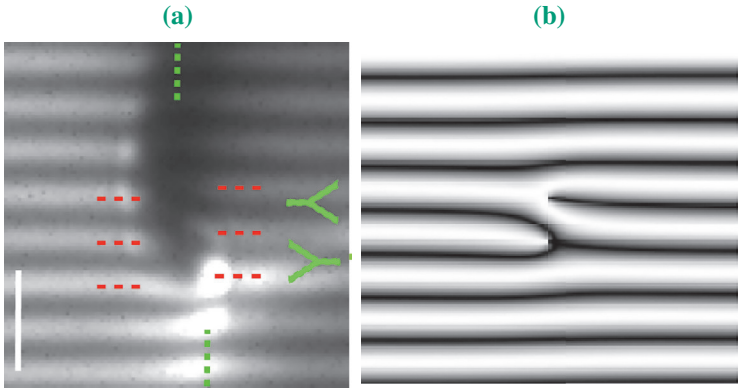

Fig. 3. **(a)** Interferograms obtained at off-Bragg condition with offset angle of $\Delta\theta$ = 10″. Two Y-shaped fork patterns bridging the dark line, near the image center, were observed with reversed orientations and with the separation of the amount of shear. This dark area contains the contributions of the dark center of vortices. Upper and lower green dotted lines are likely related to basal plane dislocations. The exposure time is 20 s and the scale bar is 10 μm. **(b)** Simulated interferogram in the kinematical diffraction regime.

Yoshiki Kohmura[a,*] and Kenji Ohwada[b]

[a] RIKEN SPring-8 Center
[b] Synchrotron Radiation Research Center, National Institutes for Quantum Science and Technology (QST)

*Email: yoshiki.kohmura@riken.jp

References

[1] H. Yamaguchi and H. Matsuhata: J. Electron. Mater. **39** (2010) 715.
[2] Y. Kohmura *et al.*: Opt. Express **28** (2020) 24115.
[3] Y. Kohmura: SPring-8/SACLA Research Frontiers 2020, p. 50.
[4] *Y. Kohmura, K. Ohwada, N. Kakiuchi, K. Sawada, T. Kaneko, J. Mizuki, M. Mizumaki, T. Watanuki and T. Ishikawa: Phys. Rev. Res.* ***5*** *(2023) L012043.*